

Addison-Wesley Wireless Communications Series

CDMA

Principles of
Spread
Spectrum
Communication



Andrew J. Viterbi

CDMA

Principles of Spread Spectrum Communication

Andrew J. Viterbi



ADDISON-WESLEY PUBLISHING COMPANY

Reading, Massachusetts · Menlo Park, California · New York · Don Mills, Ontario
Wokingham, England · Amsterdam · Bonn · Sydney · Singapore · Tokyo · Madrid
San Juan · Paris · Seoul · Milan · Mexico City · Taipei

Many of the designations used by manufacturers and sellers to distinguish their products are claimed as trademarks. Where those designations appear in this book and Addison-Wesley was aware of a trademark claim, the designations have been printed in initial caps or all caps.

The publisher offers discounts on this book when ordered in quantity for special sales. For more information please contact:

Corporate & Professional Publishing Group
Addison-Wesley Publishing Company
One Jacob Way
Reading, Massachusetts 01867

Library of Congress Cataloging-in-Publication Data

Viterbi, Andrew J.

CDMA : principles of spread spectrum communication / Andrew J. Viterbi.
p. cm.

Includes bibliographical references and index.

ISBN 0-201-63374-4

1. Code division multiple access. I. Title.

TK5103.45.V57 1995

321.3845—dc20

94-23800

CIP

Copyright © 1995 by Addison-Wesley Publishing Company

All rights reserved. No part of this publication may be reproduced, stored in a retrieval system, or transmitted, in any form, or by any means, electronic, mechanical, photocopying, recording, or otherwise, without the prior consent of the publisher. Printed in the United States of America. Published simultaneously in Canada.

Text design by Wilson Graphics & Design (Kenneth J. Wilson)

ISBN 0-201-63374-4

Text printed on recycled and acid-free paper.

1 2 3 4 5 6 7 8 9 10 MA 979695

First Printing, April 1995

CONTENTS

List of Figures and Tables xiii

Preface xvii

1 INTRODUCTION

1.1 Definition and Purpose 1

1.2 Basic Limitations of the Conventional Approach 2

1.3 Spread Spectrum Principles 4

1.4 Organization of the Text 8

2 RANDOM AND PSEUDORANDOM SIGNAL GENERATION

2.1 Purpose 11

2.2 Pseudorandom Sequences 12

2.2.1 Maximal Length Linear Shift Register Sequences 12

2.2.2 Randomness Properties of MLSR Sequences 19

2.2.3 Conclusion 22

2.3 Generating Pseudorandom Signals (Pseudonoise) from Pseudorandom Sequences 23

2.3.1 First- and Second-Order Statistics of Demodulator Output in Multiple Access Interference 26

2.3.2 Statistics for QPSK Modulation by Pseudorandom Sequences 29

2.3.3 Examples 31

2.3.4 Bound for Bandlimited Spectrum 33

2.4 Error Probability for BPSK or QPSK with Constant Signals in Additive Gaussian Noise and Interference 34

Appendix 2A: Optimum Receiver Filter for Bandlimited Spectrum 37

3 SYNCHRONIZATION OF PSEUDORANDOM SIGNALS

3.1 Purpose 39

3.2 Acquisition of Pseudorandom Signal Timing 39

3.2.1 Hypothesis Testing for BPSK Spreading 40

- 3.2.2 Hypothesis Testing for QPSK Spreading 44
- 3.2.3 Effect of Frequency Error 45
- 3.2.4 Additional Degradation When N Is Much Less Than One Period 48
- 3.3 Detection and False Alarm Probabilities 48
 - 3.3.1 Fixed Signals in Gaussian Noise ($L = 1$) 49
 - 3.3.2 Fixed Signals in Gaussian Noise with Postdetection Integration ($L > 1$) 50
 - 3.3.3 Rayleigh Fading Signals ($L \geq 1$) 51
- 3.4 The Search Procedure and Acquisition Time 52
 - 3.4.1 Single-Pass Serial Search (Simplified) 53
 - 3.4.2 Single-Pass Serial Search (Complete) 56
 - 3.4.3 Multiple Dwell Serial Search 58
- 3.5 Time Tracking of Pseudorandom Signals 60
 - 3.5.1 Early-Late Gate Measurement Statistics 61
 - 3.5.2 Time Tracking Loop 63
- 3.6 Carrier Synchronization 67
- Appendix 3A: Likelihood Functions and Probability Expressions 68
 - 3A.1 Bayes and Neyman-Pearson Hypothesis Testing 68
 - 3A.2 Coherent Reception in Additive White Gaussian Noise 69
 - 3A.3 Noncoherent Reception in AWGN for Unfaded Signals 70
 - 3A.4 Noncoherent Reception of Multiple Independent Observations of Unfaded Signals in AWGN 72
 - 3A.5 Noncoherent Reception of Rayleigh-Faded Signals in AWGN 74

- 4 MODULATION AND DEMODULATION OF SPREAD SPECTRUM SIGNALS IN MULTIPATH AND MULTIPLE ACCESS INTERFERENCE**
 - 4.1 Purpose 77
 - 4.2 Chernoff and Bhattacharyya Bounds 77
 - 4.2.1 Bounds for Gaussian Noise Channel 79
 - 4.2.2 Chernoff Bound for Time-Synchronous Multiple Access Interference with BPSK Spreading 80
 - 4.2.3 Chernoff Bound for Time-Synchronous Multiple Access Interference with QPSK Spreading 82
 - 4.2.4 Improving the Chernoff Bound by a Factor of 2 83

- 4.3 Multipath Propagation: Signal Structure and Exploitation 84
- 4.4 Pilot-Aided Coherent Multipath Demodulation 87
 - 4.4.1 Chernoff Bounds on Error Probability for Coherent Demodulation with Known Path Parameters 92
 - 4.4.2 Rayleigh and Rician Fading Multipath Components 93
- 4.5 Noncoherent Reception 96
 - 4.5.1 Quasi-optimum Noncoherent Multipath Reception for M -ary Orthogonal Modulation 97
 - 4.5.2 Performance Bounds 105
- 4.6 Search Performance for Noncoherent Orthogonal M -ary Demodulators 108
- 4.7 Power Measurement and Control for Noncoherent Orthogonal M -ary Demodulators 113
 - 4.7.1 Power Control Loop Performance 116
 - 4.7.2 Power Control Implications 118
- Appendix 4A: Chernoff Bound with Imperfect Parameter Estimates 120

5 CODING AND INTERLEAVING

- 5.1 Purpose 123
- 5.2 Interleaving to Achieve Diversity 123
- 5.3 Forward Error Control Coding—Another Means to Exploit Redundancy 126
 - 5.3.1 Convolutional Code Structure 127
 - 5.3.2 Maximum Likelihood Decoder—Viterbi Algorithm 132
 - 5.3.3 Generalization of the Preceding Example 139
- 5.4 Convolutional Code Performance Evaluation 140
 - 5.4.1 Error Probability for Tailed-off Block 140
 - 5.4.2 Bit Error Probability 142
 - 5.4.3 Generalizations of Error Probability Computation 143
 - 5.4.4 Catastrophic Codes 149
 - 5.4.5 Generalization to Arbitrary Memoryless Channels—Coherent and Noncoherent 151
 - 5.4.6 Error Bounds for Binary-Input, Output-Symmetric Channels with Integer Metrics 152
- 5.5 A Near-Optimal Class of Codes for Coherent Spread Spectrum Multiple Access 155
 - 5.5.1 Implementation 155

- 5.5.2 Decoder Implementation 157
- 5.5.3 Generating Function and Performance 159
- 5.5.4 Performance Comparison and Applicability 164
- 5.6 Orthogonal Convolutional Codes for Noncoherent Demodulation of Rayleigh Fading Signals 167
 - 5.6.1 Implementation 167
 - 5.6.2 Performance for L -Path Rayleigh Fading 168
 - 5.6.3 Conclusions and Caveats 171
- Appendix 5A: Improved Bounds for Symmetric Memoryless Channels and the AWGN Channel 173
- Appendix 5B: Upper Bound on Free Distance of Rate $1/n$ Convolutional Codes 176

6 CAPACITY, COVERAGE, AND CONTROL OF SPREAD SPECTRUM MULTIPLE ACCESS NETWORKS

- 6.1 General 179
- 6.2 Reverse Link Power Control 182
- 6.3 Multiple Cell Pilot Tracking and Soft Handoff 183
- 6.4 Other-Cell Interference 185
 - 6.4.1 Propagation Model 185
 - 6.4.2 Single-Cell Reception—Hard Handoff 186
 - 6.4.3 Soft Handoff Reception by the Better of the Two Nearest Cells 189
 - 6.4.4 Soft Handoff Reception by the Best of Multiple Cells 193
- 6.5 Cell Coverage Issues with Hard and Soft Handoff 196
 - 6.5.1 Hard Handoff 196
 - 6.5.2 Soft Handoff 198
- 6.6 Erlang Capacity of Reverse Links 199
 - 6.6.1 Erlang Capacity for Conventional Assigned-Slot Multiple Access 199
 - 6.6.2 Spread Spectrum Multiple Access Outage—Single Cell and Perfect Power Control 203
 - 6.6.3 Outage with Multiple-Cell Interference 207
 - 6.6.4 Outage with Imperfect Power Control 208
 - 6.6.5 An Approximate Explicit Formula for Capacity with Imperfect Power Control 212
 - 6.6.6 Designing for Minimum Transmitted Power 214
 - 6.6.7 Capacity Requirements for Initial Accesses 215

- 6.7 Erlang Capacity of Forward Links 218
 - 6.7.1 Forward Link Power Allocation 218
 - 6.7.2 Soft Handoff Impact on Forward Link 222
 - 6.7.3 Orthogonal Signals for Same-Cell Users 224
- 6.8 Interference Reduction with Multisectored and Distributed Antennas 227
- 6.9 Interference Cancellation 229
- 6.10 Epilogue 232

- References and Bibliography 235

- Index 239

In Chapters 2 to 5, this book covers all aspects of spread spectrum transmission over a physical multiple-access channel: signal generation, synchronization, modulation, and error-correcting coding of direct-sequence spread spectrum signals. Chapter 6 relates these physical layer functions to link and network layer properties involving cellular coverage, Erlang capacity, and network control. This outline is unusual in bringing together several wide-ranging technical disciplines, rarely covered in this sequence and in one text. However, the presentation is well integrated by a number of unifying threads. First, the entire text is devoted to the concept of universal frequency reuse by multiple users of multiple cells. Also, two fundamental techniques are used in a variety of different forms throughout the text. The first is the finite-state machine representation of both deterministic and random sequences; the second is the use of simple, elegant upper bounds on the probabilities of a wide range of events related to system performance.

However, given the focus on simultaneous wideband transmission for all users over a common frequency spectrum, the text purposely omits two important application areas: narrowband modulation and coding methods, including multipoint signal constellations and trellis codes; and frequency hopped multiple access, where modulation waveforms are instantaneously narrowband over the duration of each hop. It also generally avoids digressions into principles of information theory. In short, although the material covered through Chapter 5 mostly also applies to narrowband digital transmission systems, the book mainly covers topics that apply to wideband spread spectrum multiple access.

Three motivating forces drove me to write this book. It began with my three decades of teaching within the University of California system. There, keeping with the healthy trend in communication engineering courses, I tried to make theory continually more pertinent to applications. Then there was the fulfillment of a voluntary commission for the Marconi Foundation, which honored me with a Marconi Fellowship award in 1990. Most important was my participation in a significant technological achievement in communication system evolution: the implementation, demonstration, and standardization of a digital cellular spread spectrum code-division multiple access (CDMA) system. Adopted in 1993 by the Telecommunication Industry Association, the CDMA standard IS-95 is the embodiment of many of the principles presented in this text. Although this book is not meant solely for this purpose, it does explain and justify many of the techniques contained in the standard. I emphasize, however, that my goal is to present the principles underlying spread spectrum communication, most but not all of which apply to this standard. It is not to describe in detail how the principles were applied. This is left to the

The pilot sequence can be searched by the hypothesis testing device of Figure 3.1 with time (delay) hypotheses separated by a fraction of a chip T_c . However, once the first strong component is found, the entire search window for all components can be limited to typically a few tens of chip times, representing the total delay dispersion of the multipath propagation. The pilot pseudorandom sequence is unmodulated, and the carrier frequency is assumed to be accurately tracked. Thus, the number of chips used for estimation can be made as large as desired, limited only by the rate of change of amplitude and phase. Also, unlike the last chapter where the initial acquisition search ended when the correct hypothesis was detected, the search here will not end. Once a path is detected and verified, the search continues indefinitely, since new multipath components will appear and old ones disappear frequently, particularly for users in motion. Once found, the component sequence timing must be tracked by an early-late gate, both to refine the time estimate and to adjust for distance and velocity of users in motion.

We will explore this mechanization more fully. However, we first note that whereas the multipath propagation model of Figure 4.1 has long been accepted in the communication theory literature, it has been traditionally associated with a static receiver, in which it was assumed that each of the components (and even their number, L) remained at a constant delay, although their amplitudes and phases might vary. Employing a receiver that takes a static number of paths, in place of the varying number assumed here, complicates the form of the optimum receiver: L must generally be taken to be larger than if only the currently active path delays are being demodulated. Also, with a static receiver, motion causes a transition from one delay path to another with possible discontinuity of amplitude and phase.

In the next section we explore the optimum pilot-aided demodulator based on tracking each multipath component. In the following subsection, we consider its performance.

4.4 Pilot-Aided Coherent Multipath Demodulation

A pilot sequence for determining multipath component characteristics is well justified for one-to-many transmission channels, such as the forward (down-) link from a base station to multiple users. This is because the same pilot sequence is shared among the k_u users controlled by that base station. For the same reason, the energy devoted to the pilot can be greater than that devoted to the individual users. Thus, if $X_k(t)$ given in (4.24) is the received signal for the k th user, let $X_0(t)$ be the unmodulated pilot

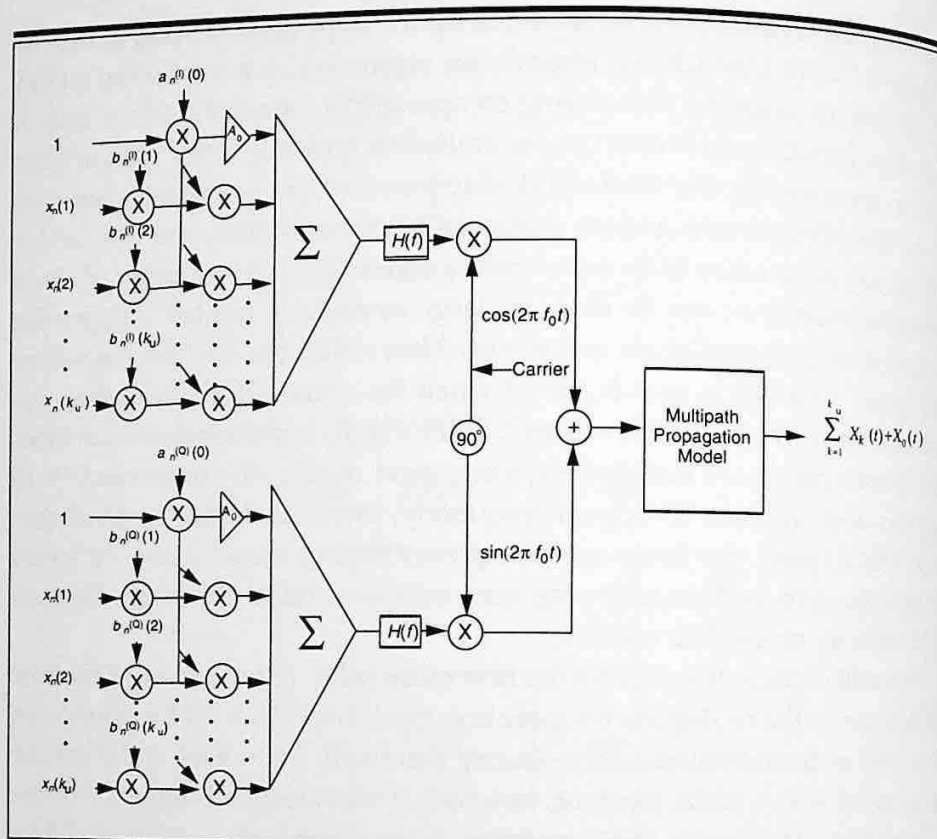


Figure 4.2 Multiuser (base station) modulator and multipath channel.

signal, so that $x_n(0) = 1$ for all n . Also, we assume that the pilot's pseudo-random sequence is shared by all users by multiplying the pilot pseudo-random (± 1) sequence with all the user-specific sequences (Figure 4.2). Hence, the received signal containing k_u users and a pilot sequence, all originating from a common base station, will be

$$X_0(t) + \sum_{k=1}^{k_u} X_k(t).$$

Here, $X_k(t)$ is given by (4.24) for $k = 1, 2, \dots, k_u$, but $X_0(t)$ is further scaled by A_0 , the additional gain allotted to the pilot signal.

As shown in Figure 4.2, $a_n^{(1)}(0)$ and $a_n^{(Q)}(0)$ are the pilot's QPSK spreading sequence. The users' sequences are the product⁵ of those of the pilot

⁵ The reason for multiplying the user sequence by the pilot sequence is to identify the user with the particular base station that is handling the call.

and of the user-specific sequences $b_n^{(I)}(k)$ and $b_n^{(Q)}(k)$. That is,

$$\begin{aligned} a_n^{(I)}(k) &= a_n^{(I)}(0)b_n^{(I)}(k), \\ a_n^{(Q)}(k) &= a_n^{(Q)}(0)b_n^{(Q)}(k), \quad k = 1, 2, \dots, k_u. \end{aligned} \quad (4.25)$$

Furthermore, the timing of all individual users is locked to that of the pilot sequence, so that the multipath delays need only be searched on the pilot sequence.

The optimum demodulator structure for L multipath propagation paths (as assumed in Figure 4.1) is known as a Rake receiver [Price and Green, 1958]. It was first implemented in static form in the late 1950s. This is shown in Figure 4.3 for the k th user. Figure 4.3a consists of the parallel combination of L elements, one of which is shown in Figure 4.3b. Each multipath component demodulator is called a "finger" of the rake. The pilot sequence tracking loop of a particular demodulator is started by the timing delay estimation of a given path, as determined by the pilot's pseudorandom sequence searcher. This is then used to remove the pilot QPSK spreading, giving rise to the quadrature outputs (Figure 4.3):

$$\begin{aligned} \sqrt{E_c} [A_0 + x_n(k)b_n^{(I)}(k)]\alpha_\ell \cos \phi_\ell + \nu_n^{(I)}, \\ \sqrt{E_c} [A_0 + x_n(k)b_n^{(Q)}(k)]\alpha_\ell \sin \phi_\ell + \nu_n^{(Q)}. \end{aligned}$$

A_0 is the pilot gain, and $\nu_n^{(I)}$ and $\nu_n^{(Q)}$ are the contributions of all other (uncorrelated) multipath components as well as those of all other users. From this the relative path values $\alpha_\ell \cos \phi_\ell$ and $\alpha_\ell \sin \phi_\ell$ can be estimated by simply averaging over an arbitrary number of chips, N_p . This number should be as large as possible without exceeding the period over which α_ℓ and ϕ_ℓ remain relatively constant.

The optimum (maximum likelihood) demodulator forms the weighted, phase-adjusted, and delay-adjusted sum of the L components. This amounts to taking the inner product of the modulated received I and Q components with the I and Q unmodulated component magnitude estimates $\hat{\alpha}_\ell \cos \hat{\phi}_\ell$ and $\hat{\alpha}_\ell \sin \hat{\phi}_\ell$. The result for the n th chip of the ℓ th path, after multiplication by the quadrature-user-specific pseudorandom sequences as shown in Figure 4.3b, is

$$\begin{aligned} y_{en}(k) &= \sqrt{E_c} x_n(k) \hat{\alpha}_\ell \alpha_\ell \cos(\phi_\ell - \hat{\phi}_\ell) \\ &\quad + \hat{\alpha}_\ell (\nu_n^{(I)} \cos \hat{\phi}_\ell + \nu_n^{(Q)} \sin \hat{\phi}_\ell). \end{aligned} \quad (4.26)$$

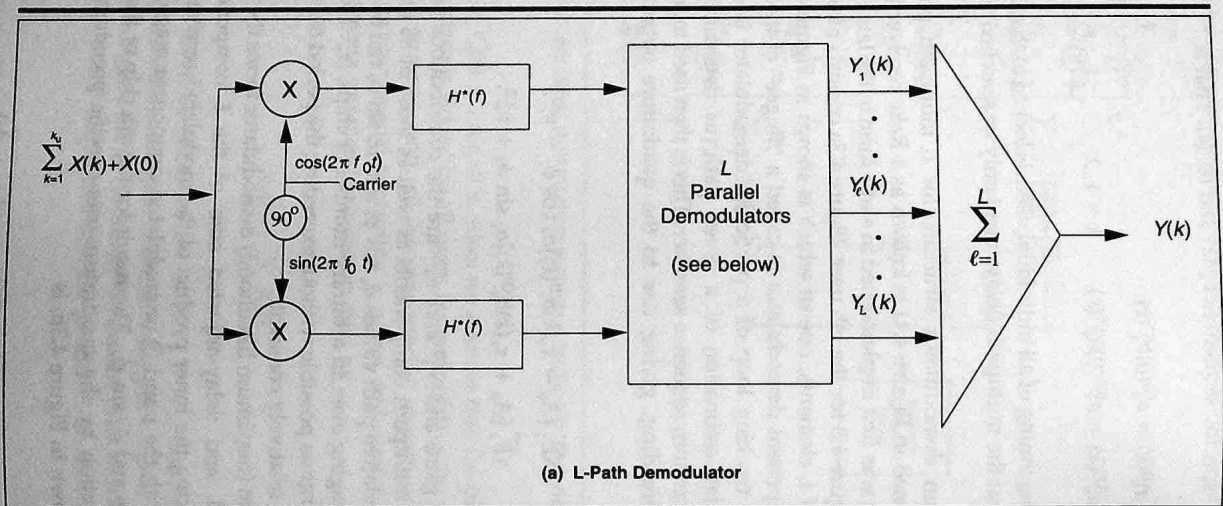


Figure 4.3 Pilot-aided coherent Rake demodulator for multipath propagation. (a) L-path demodulator.

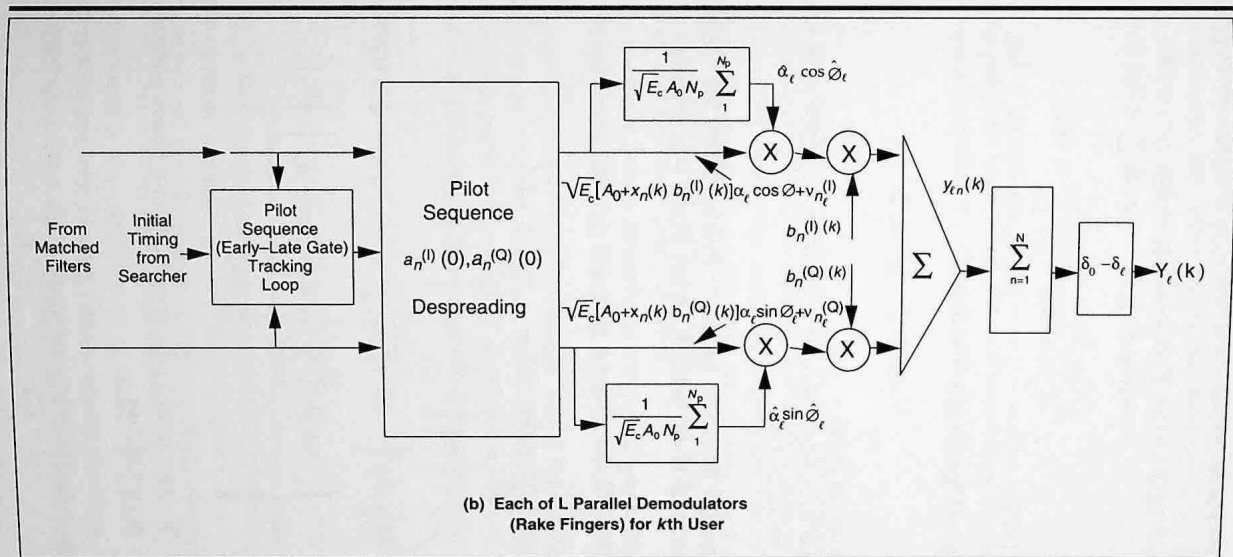


Figure 4.3 (b) Each of L parallel demodulators (Rake fingers) for k th user.

Summing over the N chips over which $x_n(k)$ is constant (± 1), we have

$$Y_\ell(k) = \pm N\sqrt{E_c} \alpha_\ell \hat{\alpha}_\ell \cos(\phi_\ell - \hat{\phi}_\ell) + \hat{\alpha}_\ell [\cos \hat{\phi}_\ell \sum v_n^{(1)} + \sin \hat{\phi}_\ell \sum v_n^{(0)}]. \quad (4.27)$$

Thus,

$$E[Y_\ell(k) | x_n(k) = -1] = -N[\sqrt{E_c} \alpha_\ell \hat{\alpha}_\ell \cos(\phi_\ell - \hat{\phi}_\ell)], \quad (4.28a)$$

with a change of sign if $x_n(k) = +1$, and

$$\text{Var}[Y_\ell(k)] = N\hat{\alpha}_\ell^2 I_0 / 2, \quad (4.28b)$$

where I_0 is given in (4.16).

We proceed to obtain Chernoff bounds on the error probability using the methods of Section 4.2.

4.4.1 Chernoff Bounds on Error Probability for Coherent Demodulation with Known Path Parameters

Initially, conditioning on known amplitudes α_ℓ and phases ϕ_ℓ , we obtain the Chernoff bound,

$$\begin{aligned} P_E(\boldsymbol{\alpha}, \boldsymbol{\phi}; k) &= \Pr \left[\sum_{\ell=1}^L Y_\ell(k) > 0 \mid \boldsymbol{\alpha}, \boldsymbol{\phi}, x(k) = -1 \right] \\ &< \text{Min}_{\rho > 0} E \left(\exp \left[\rho \sum_{\ell=1}^L Y_\ell(k) \right] \mid \boldsymbol{\alpha}, \boldsymbol{\phi}, x(k) = -1 \right) \\ &= \text{Min}_{\rho > 0} \exp \left[-\rho N \sqrt{E_c(k)} \sum_{\ell=1}^L \alpha_\ell \hat{\alpha}_\ell \cos(\phi_\ell - \hat{\phi}_\ell) + \rho^2 N \sum_{\ell=1}^L \hat{\alpha}_\ell^2 I_0 / 4 \right] \\ &= \exp \left\{ -\frac{NE_c(k) \left[\sum_{\ell=1}^L \alpha_\ell \hat{\alpha}_\ell \cos(\phi_\ell - \hat{\phi}_\ell) \right]^2}{\sum_{\ell=1}^L \hat{\alpha}_\ell^2 I_0} \right\}. \end{aligned} \quad (4.29)$$

If we neglect the inaccuracy in the amplitude and phase estimates, taking $\hat{\phi}_\ell = \phi_\ell$, $\hat{\alpha}_\ell = \alpha_\ell$, we obtain

$$\begin{aligned} P_E(k) &< \exp \left[-\sum_{\ell=1}^L \alpha_\ell^2 NE_c(k) / I_0 \right] \\ &= \prod_{\ell=1}^L \exp[-\alpha_\ell^2 NE_c(k) / I_0] \quad (\text{perfect estimates}). \end{aligned} \quad (4.30)$$

Further, it is shown in Appendix 4A that if we do not assume exact phase and amplitude estimates, but rather estimates based on N_p unmodulated chips of a pilot whose chip energy is $A_0^2 E_c$ (see Figure 4.3), the error probability is bounded by

$$P_E(k) < \prod_{\ell=1}^L \frac{\exp[-\alpha_\ell^2 N E_c(k)/I_0]}{1 - [N/(A_0^2 N_p)]}. \quad (4.31)$$

Generally, if the paths are known and the total received energy per chip is $E_c(k)$, then we may normalize the relative path gains so that

$$\sum_{\ell=1}^L \alpha_\ell^2 = 1.$$

Thus, for fixed amplitude and phase multipath, the performance bound with perfect estimates, (4.30), is the same as for a single-component signal, if energy is taken as the sum of the component energies. The explanation is simple: When the multipath amplitudes and phases are known, the optimal receiver operates as a matched filter to the combination of the transmitter filter and the (multipath) channel.

4.4.2 Rayleigh and Rician Fading Multipath Components

Now we no longer assume constant amplitude. We let the multipath component amplitudes be random variables, mutually independent because we assume that each path's attenuation is unrelated to that of all others. Then the error probability for perfect estimates becomes

$$\begin{aligned} P_E &= E[P_E(\alpha_1, \dots, \alpha_L)] < E \left[\prod_{\ell=1}^L \exp(-\alpha_\ell^2 N E_c / I_0) \right] \\ &= \prod_{\ell=1}^L E[\exp(-\alpha_\ell^2 E_s / I_0)] \triangleq \prod_{\ell=1}^L Z_\ell \triangleq Z. \end{aligned} \quad (4.32)$$

Here, $E_s \triangleq N E_c$ is the N -chip symbol energy, and the expectations are with respect to the random variables α_ℓ . We drop the user index k for convenience. We also assume perfect estimates, although by scaling all Z_ℓ by the denominator of (4.31), we may also obtain a bound for imperfect estimates.

If each component is the combination of many reflections arriving at nearly the same delay but with random phases, we can take the α_ℓ variable to be Rayleigh-distributed. Then the probability density function of α_ℓ is

$$p(\alpha) = \frac{2\alpha e^{-\alpha^2/\sigma_\ell^2}}{\sigma_\ell^2}, \quad \alpha > 0. \quad (4.33a)$$

Or, letting $\beta_\ell = \alpha_\ell^2$, we obtain the chi-squared density,

$$p(\beta) = \frac{e^{-\beta/\sigma_\ell^2}}{\sigma_\ell^2}, \quad \beta > 0, \quad (4.33b)$$

where $\sigma_\ell^2 = E[\beta_\ell] = E[\alpha_\ell^2]$.

Thus, for Rayleigh-distributed attenuations,

$$\begin{aligned} Z_\ell &= E[e^{-\beta_\ell E_s/I_0}] = \int_0^\infty \frac{1}{\sigma_\ell^2} \exp\left[\frac{-\beta}{\sigma_\ell^2} \left(\frac{E_s}{I_0} \sigma_\ell^2 + 1\right)\right] d\beta \\ &= \frac{1}{1 + \sigma_\ell^2 E_s/I_0}. \end{aligned} \quad (4.34)$$

Letting

$$\bar{E}_{s_\ell} = \bar{\beta}_\ell E_s = \sigma_\ell^2 E_s,$$

this can be written as

$$Z_\ell = \frac{1}{1 + \bar{E}_{s_\ell}/I_0} \quad (\text{Rayleigh fading component}). \quad (4.35)$$

If the component is the combination of a specular component and a Rayleigh component, the probability density function of α_ℓ becomes Rician. Its square β_ℓ becomes noncentral chi-squared,

$$p(\beta_\ell) = \frac{e^{-(\beta_\ell + \gamma_\ell)/\sigma_\ell^2}}{\sigma_\ell^2} \mathcal{I}_0(2\sqrt{\gamma_\ell \beta_\ell}/\sigma_\ell^2). \quad (4.36)$$

Then

$$\begin{aligned} Z_\ell &= E[e^{-\beta_\ell E_s/I_0}] \\ &= \int_{-\infty}^\infty \exp\left[-\frac{\gamma_\ell + \beta_\ell(1 + \sigma_\ell^2 E_s/I_0)}{\sigma_\ell^2}\right] \mathcal{I}_0\left(2\frac{\sqrt{\gamma_\ell \beta_\ell}}{\sigma_\ell^2}\right) d\beta_\ell/\sigma_\ell^2 \\ &= \frac{1}{1 + \sigma_\ell^2 E_s/I_0} \exp\left(-\frac{\gamma_\ell E_s/I_0}{1 + \sigma_\ell^2 E_s/I_0}\right) \quad (\text{Rician fading component}). \end{aligned} \quad (4.37)$$

Note that this reduces to the Rayleigh fading result (4.34) when $\gamma_\ell = 0$, and to the known amplitude and phase result when $\sigma_\ell^2 = 0$.

Finally, suppose that the L multipath components are all Rayleigh of equal average strength, so that

$$\sigma_\ell^2 = \sigma^2 \quad \text{for all } \ell,$$

and therefore, for each component,

$$\bar{E}_{s_\ell} = \sigma_\ell^2 E_s = \sigma^2 E_s = \bar{E}_s.$$

Then, letting the random variable

$$x = \sum_{\ell=1}^L \alpha_\ell^2 E_s = \sum_{\ell=1}^L \beta_\ell E_s,$$

it is easily shown (see Appendix 3A.5) that since the individual fading variables are all independent,

$$p(x) = \frac{x^{L-1} e^{-x/\bar{E}_s}}{(L-1)! (\bar{E}_s)^L}, \quad (4.38)$$

which is L th-order chi-squared. It follows from (4.34) that, in this case,

$$\bar{P}_E < Z \triangleq \prod_{\ell=1}^L Z_\ell = \left[\frac{1}{1 + (\sigma^2 E_s / I_0)} \right]^L = \left[\frac{1}{1 + (\bar{E}_s / I_0)} \right]^L. \quad (4.39)$$

We may rewrite (4.39) as

$$\bar{P}_E < \exp[-\ln(1/Z)],$$

where

$$\ln(1/Z) = L \ln[1 + (\bar{E}_s / I_0)]. \quad (4.40)$$

From (4.40) we obtain Figure 4.4: a plot of the ratio⁶ of the total average symbol energy-to-interference density $L\bar{E}_s/I_0$ over that required for an unfaded Gaussian channel to achieve a given exponent value, $\ln(1/Z)$. Note from (4.9) or (4.32) that for the latter channel, $\ln(1/Z) = E_s/I_0$. Thus, this is the average excess energy (in decibels) required by this degraded channel to achieve the same performance as for an unfaded signal in additive Gaussian noise.

⁶ All quantities are in decibels and hence are logarithmic functions. Thus, this ratio is actually the excess energy, in decibels, required for the faded channel over that required for the unfaded AWGN channel.

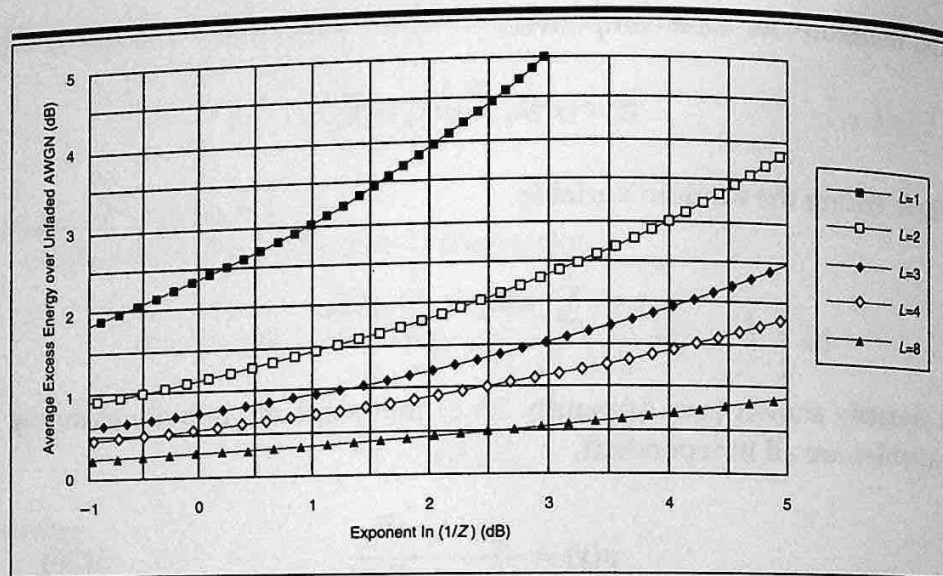


Figure 4.4 Required excess energy (dB) for L equal-strength multipath fading relative to unfaded coherent AWGN.

Note that as $L \rightarrow \infty$ (so that each component's average energy $\bar{E}_s \rightarrow 0$, but $L\bar{E}_s$ is finite), the bound approaches

$$\bar{P}_E < e^{-L\bar{E}_s/I_0},$$

so that the excess energy approaches zero. This shows that with an asymptotically large number of independent Rayleigh components, performance approaches that of unfaded propagation. This is an extreme and unrealistic example of the beneficial effect of independent diversity components. We shall return to these results in Chapter 5 when we consider interleaving, with delay, to produce more independent components.

4.5 Noncoherent Reception

Transmission of a pilot is very valuable for initial acquisition and time tracking. It is also valuable for obtaining good amplitude and phase estimates, making possible quasi-optimum coherent reception and weighted combining of multipath components. Unfortunately, it is a luxury that may not always be affordable, particularly on the many-to-one reverse (up-) link from each of the multiple access users to the base station. For this purpose, inserting in each individual user's signal a pilot whose power is greater than the data-modulated portion of the signal reduces

station may be estimated a priori to lie between 3 and 7 dB, according to the analyses in Chapters 4 and 5. However, conditions will vary according to the multipath fading environment, particularly if many paths are involved. Thus, as noted in Section 4.7, it is useful to add a power control mechanism called an *outer loop*, which adjusts the desired E_b/I_0 level according to the individual user's error rate measured at the base station. This then guarantees a given error rate per coded voice frame or message packet (typically set at or below 1%). However, the resulting E_b/I_0 parameter, which is already a log-normal random variable—or normal in decibels—because of power control inaccuracy, will have greater variability, manifested as a larger standard deviation of its normally distributed decibel measure. Thus, while Section 4.7 arrives at a typical standard deviation for the closed-loop system between 1.1 and 1.5 dB, the standard deviation caused by the outer loop variations is of the same order of magnitude. Hence, the combination of these two independent components leads to an estimate of total standard deviation on the order of 1.5 to 2.1 dB. It has been measured experimentally [Viterbi and Padovani, 1992; Padovani, 1994] to be between 1.5 and 2.5 dB. We shall assess the effect of variability on capacity in Section 6.6.

6.3 Multiple Cell Pilot Tracking and Soft Handoff

The forward link for each cell or sector generally employs a pilot modulated only by the cell-specific, or sector-specific, pseudorandom sequence, added or multiplexed with the voice or data traffic. This is described in Chapter 4 and shown in Figure 4.2. The pilot provides for time reference and phase and amplitude tracking. It also can be used to identify newly available pilots in adjacent cells or sectors. Specifically, while a user is tracking the pilot of a particular cell, it can be searching for pilots of adjacent cells (using the searching mechanism of its multipath rake receiver). To make this simple and practical, all pilot pseudorandom sequences can use the same maximum length generator sequence, with different initial vectors and hence timing offsets. The relative time-offsets of pilots for neighboring cells and sectors are either known a priori or broadcast to all users of the given cell or sector on a separate

control loop performance. One simple method is to puncture (see Section 5.3.3) the forward link code infrequently (e.g., one symbol in 12) and dedicate the punctured symbols to uncoded transmission of commands. The punctured code is then reduced in rate (e.g., by the factor 11/12 if one in 12 symbols is punctured). Its performance is slightly degraded.

CDMA channel, employing its own pseudorandom sequence or time-offset.

Once a new pilot is detected by the searcher and found to have sufficient signal strength (usually relative to the first pilot already being tracked), the mobile will signal this event to its original base station. This in turn will notify the switching center, which enables the second cell's base station to both send and receive the same traffic to and from the given mobile. This process is called *soft handoff*. For forward link transmission to the mobile, the Rake demodulator (Figure 4.3) demodulates both cells' transmission in two fingers of the rake and combines them coherently, with appropriate delay adjustments, just as is done for time-separated multipath components. For the reverse link, normally each base station demodulates and decodes each frame or packet independently. Thus, it is up to the switching center to arbitrate between the two base stations' decoded frames.² Soft handoff operation has many advantages. Qualitatively, transition of a mobile between cells is much smoother: The second cell can be brought into use gradually, starting early in the transition of a mobile from one cell to its neighbor cell. Similarly, when the first cell's signal is so weak relative to the second that it cannot be demodulated and decoded correctly, it will be dropped either in response to the mobile's pilot strength measurement or by action of the first cell. Moreover, for any given frame, the better cell's decision will generally be used, with no need to enable a new cell or disable an old one as in classical "hard" handoff. In fact, to avoid frequent handoffs on the boundary between cells (which require excessive control signaling), systems with hard handoff only enable a second cell when its signal strength is considerably above (e.g., 6 dB) that of the first cell. This further degrades performance on the boundary.

Most importantly, however, soft handoff considerably increases both the capacity of a heavily loaded multicellular system and the coverage (area size) of each individual cell in a lightly loaded system. We shall demonstrate this quantitatively, following Viterbi, Viterbi, Gilhousen, and Zehavi [1994]. It is first necessary to determine the mutual interference among cells of a multicellular system.

² Generally, each frame is provided with an error-detecting code (consisting of a moderate number, c , of check bits at the tail end of the frame) which allows detection of one or more errors with probability on the order of $1-2^{-c}$ [Wolf *et al.*, 1982].

CDMA

Principles of Spread Spectrum Communication

Spread spectrum multiple access communication, known commercially as CDMA (Code Division Multiple Access), is a driving technology behind the rapidly advancing personal communications industry. Its greater bandwidth efficiency and multiple access capabilities make it the leading technology for relieving spectrum congestion caused by the explosion in popularity of cellular mobile and fixed wireless telephones and wireless data terminals.

CDMA has been adopted by the Telecommunications Industry Association (TIA) as a wireless standard. As an electrical or communications engineer, you must acquire a thorough grasp of CDMA fundamentals in order to develop systems, products, and services for this demanding but rewarding market.

Written by a leader in the creation of CDMA and an internationally recognized authority on wireless digital communication, this book gives you the technical information you need. It presents the fundamentals of digital communications and covers all aspects of commercial direct-sequence spread spectrum technology, incorporating both physical-level principles and network concepts. You will find detailed information on signal generation, synchronization, modulation, and coding of direct-sequence spread spectrum signals. In addition, the book shows how these physical layer functions relate to link and network properties involving cellular coverage, Erlang capacity, and network control.

With this book, you will attain a deeper understanding of personal communications system concepts and will be better equipped to develop systems and products at the forefront of the personal wireless communications market.

Andrew J. Viterbi is a pioneer of wireless digital communications technology. He is best known as the creator of the digital decoding technique used in direct-broadcast satellite television receivers and in wireless cellular telephones, as well as numerous other applications. He is co-founder, Chief Technical Officer, and Vice Chairman of QUALCOMM Incorporated, developer of mobile satellite and wireless land communication systems employing CDMA technology. Dr. Viterbi has received numerous awards, including the Christopher Columbus Medal, the IEEE Alexander Graham Bell Award, the Marconi International Fellowship Award, the IEEE Information Society Shannon Lecturer Award, and awards from the NEC C&C Foundation and the Eduard Rhein Foundation.

Cover photo © Hewlett-Packard Company
Cover design by Simone R. Payment
♻️ Text printed on recycled paper
Corporate & Professional Publishing Group
♣️ Addison-Wesley Publishing Company



X001DMD3KJ
CDMA: PRINCIPLES OF SPREAD SPECT
Used, Good

ISBN 0-201-63374-4